

Supplementary Information

**Preparation and characterization of magnetic nanocomposite
catalysts with double Au nanoparticle layers**

Zia Ur Rahman^a, Tingting Zhang^{a,b}, Siwen Cui^{a,b}, Daoai Wang^{*a}

^aState Key Laboratory of Solid Lubrication, Lanzhou Institute of Chemical Physics, Chinese Academy of Sciences, Lanzhou 730000, China

^bUniversity of the Chinese Academy of Sciences, Beijing 100049, China

* Corresponding Authors:

E-mail: wangda@licp.cas.cn

Table S1 Kinetic constants (k) and turnover frequencies (TOF) for the reduction of p-nitrophenol by nanocomposites

Catalyst	Au (wt%)	Ag (wt%)	k (min ⁻¹)	TOF (h ⁻¹)
Fe ₃ O ₄ @SiO ₂ -Au	11.80	-	0.20	18.75
Fe ₃ O ₄ @SiO ₂ -Au@mSiO ₂	3.10	-	0.10	38.22
Fe ₃ O ₄ @SiO ₂ -Au@mSiO ₂ -Au	15.30	-	0.53	33.71
Fe ₃ O ₄ @SiO ₂ -Au@mSiO ₂ -Ag	3.40	4.10	0.95	81.52

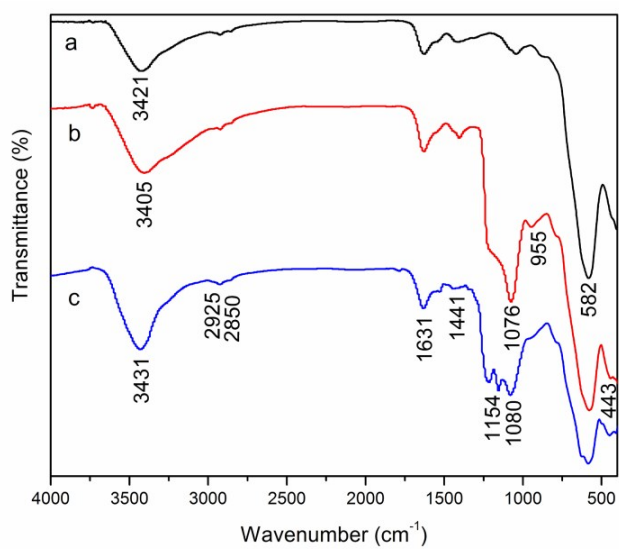


Fig. S1 FT-IR spectra of (a) Fe₃O₄, (b) Fe₃O₄@SiO₂, and (c) APTES-Fe₃O₄@SiO₂

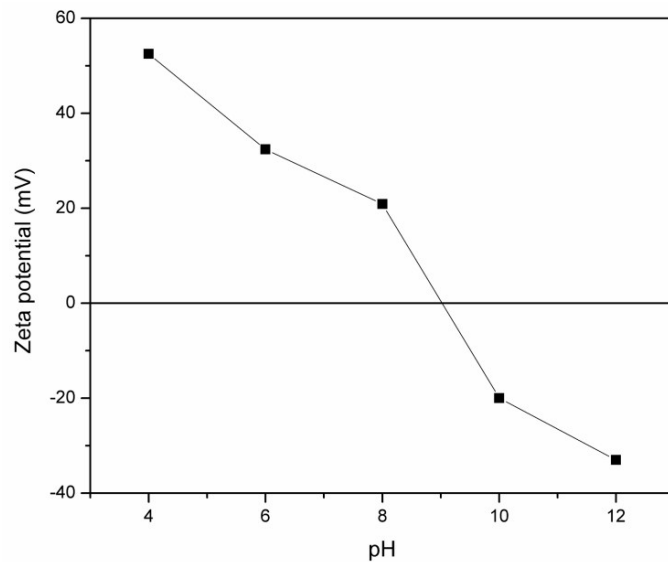


Fig. S2 Zeta potential of $\text{Fe}_3\text{O}_4@\text{SiO}_2\text{-NH}_2$ nanoparticles at different pH values indicating the presence of amine groups resulting positively charged nanoparticles.

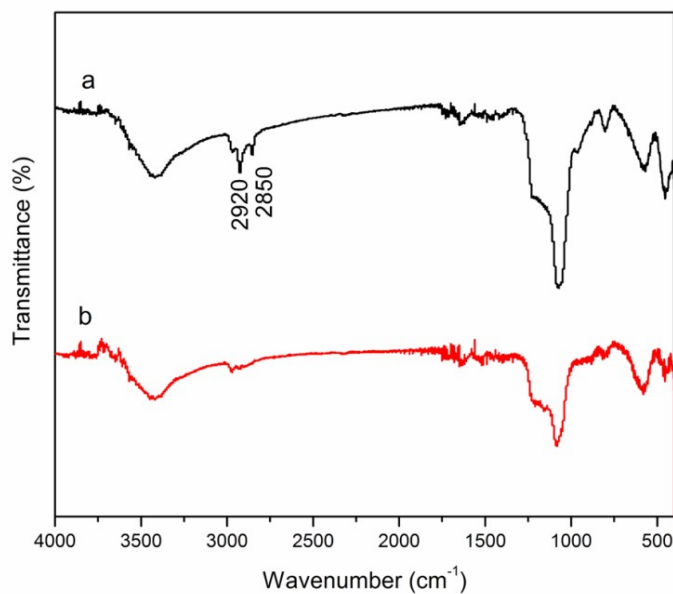


Fig. S3 FT-IR spectra of (a) nanocomposites before CTAB extraction and (b) after CTAB extraction by refluxing with acetone.

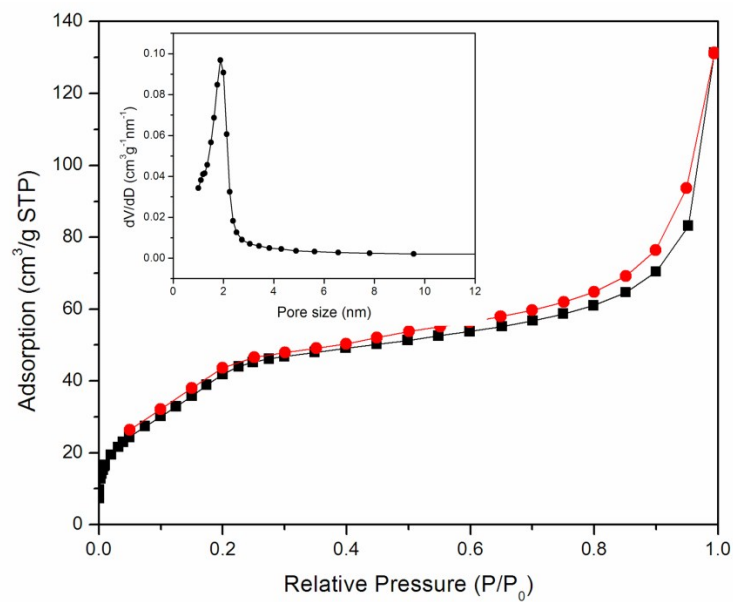


Fig. S4 N₂ adsorption-desorption isotherms and pore size distribution (inset) of Fe₃O₄@SiO₂-Au@mSiO₂ after CTAB extraction.

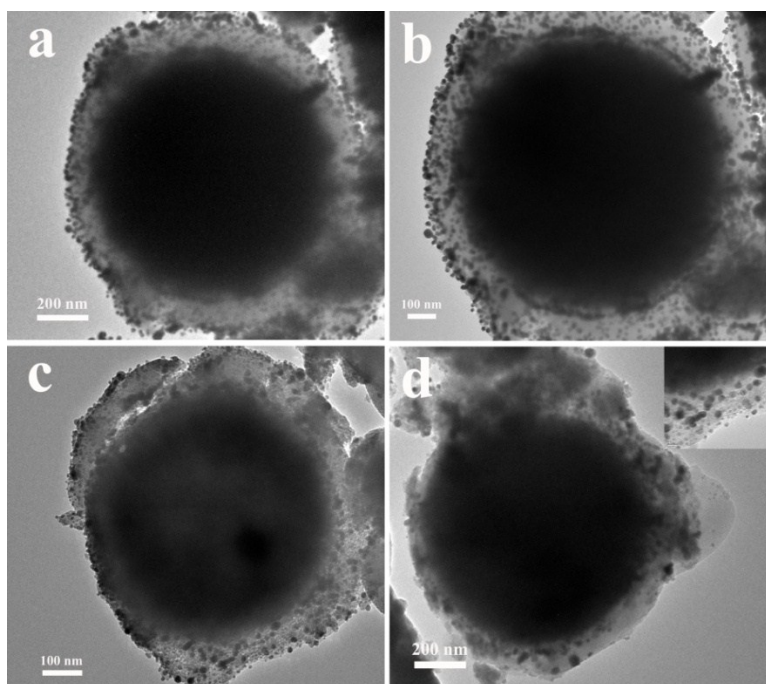


Fig. S5 TEM of (a, b) Fe₃O₄@SiO₂-Au@mSiO₂-Au and (c, d) Fe₃O₄@SiO₂-Au@mSiO₂-Ag. Inset of d shows Ag nanoparticles on the outer silica surface.

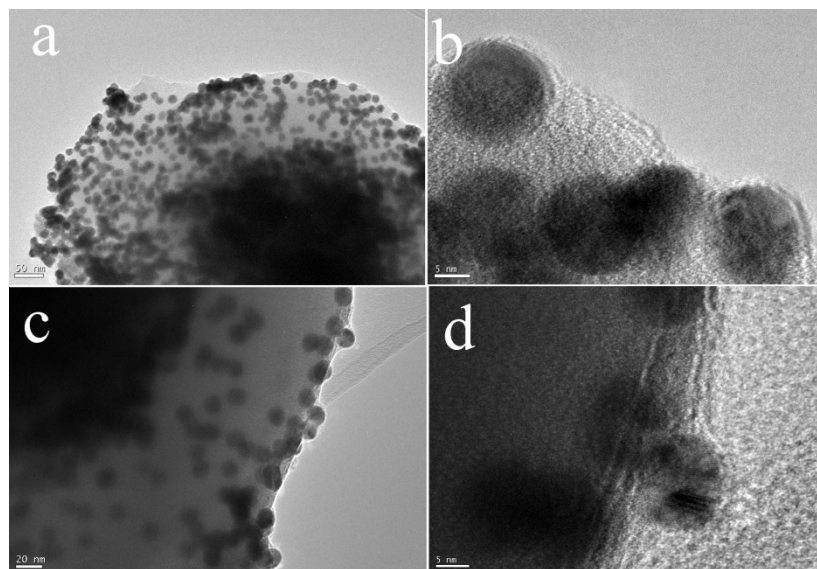


Fig. S6 HRTEM of (a, b) $\text{Fe}_3\text{O}_4@\text{SiO}_2\text{-Au@mSiO}_2\text{-Au}$ and (c, d) $\text{Fe}_3\text{O}_4@\text{SiO}_2\text{-Au@mSiO}_2\text{-Ag}$.

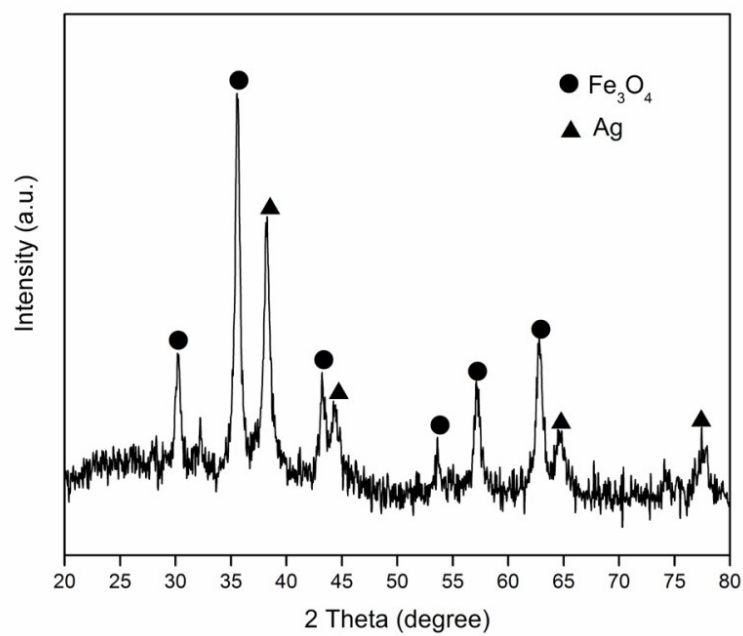


Fig. S7 The wide angle XRD patterns of $\text{Fe}_3\text{O}_4@\text{SiO}_2\text{-Au@mSiO}_2\text{-Ag}$

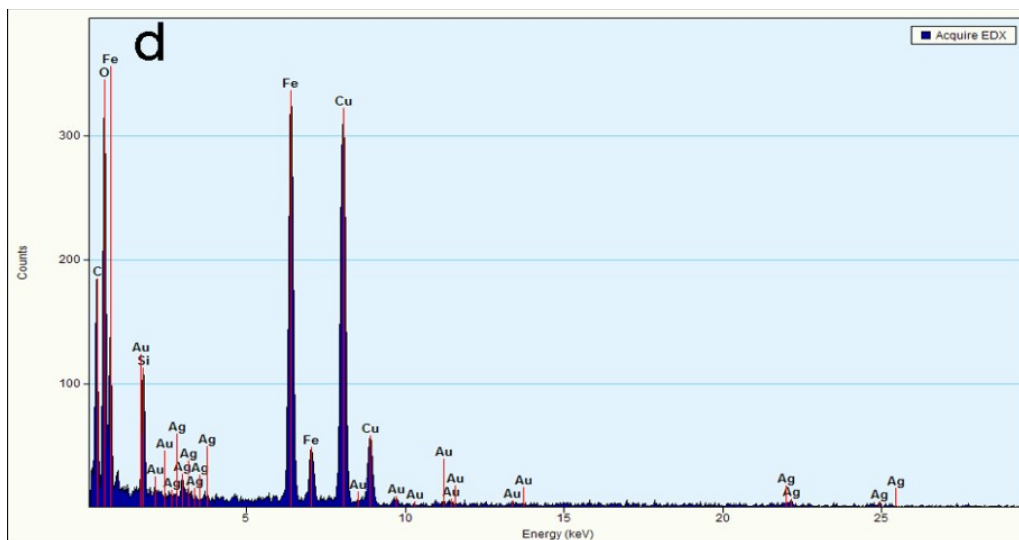


Fig. S8 EDX spectra of (a) $\text{Fe}_3\text{O}_4@\text{SiO}_2\text{-Au}$, (b) $\text{Fe}_3\text{O}_4@\text{SiO}_2\text{-Au@mSiO}_2$, (c) $\text{Fe}_3\text{O}_4@\text{SiO}_2\text{-Au@mSiO}_2\text{-Au}$, and (d) $\text{Fe}_3\text{O}_4@\text{SiO}_2\text{-Au@mSiO}_2\text{-Ag}$ indicating the presence of elements in the nanocomposites.

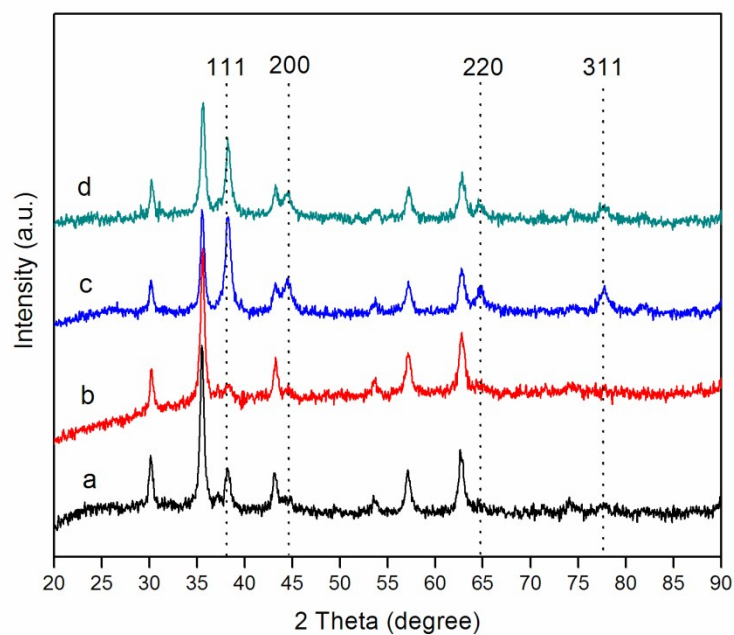


Fig. S9 The wide angle XRD patterns of (a) $\text{Fe}_3\text{O}_4@\text{SiO}_2\text{-Au}$, (b) $\text{Fe}_3\text{O}_4@\text{SiO}_2\text{-Au@mSiO}_2$, (c) $\text{Fe}_3\text{O}_4@\text{SiO}_2\text{-Au@mSiO}_2\text{-Au}$, and (d) $\text{Fe}_3\text{O}_4@\text{SiO}_2\text{-Au@mSiO}_2\text{-Ag}$ after using for 6 cycles.